Diffusion-Induced Oscillations of Extended Defects

Alexander L. Korzhenevskii

Institute for Problems of Mechanical Engineering, RAS,
Bol'shoi prosp. V. O., 61, St Petersburg, 199178, Russia

Richard Bausch

Institut für Theoretische Physik IV, Heinrich-Heine-Universität Düsseldorf,
Universitätsstrasse 1, D-40225 Düsseldorf, Germany

Rudi Schmitz

Institut für Theoretische Physik A, RWTH Aachen University, Templergraben 55, D-52056 Aachen, Germany
(Dated: September 13, 2021)

From a simple model for the driven motion of a planar interface under the influence of a diffusion field we derive a damped nonlinear oscillator equation for the interface position. Inside an unstable regime, where the damping term is negative, we find limit-cycle solutions, describing an oscillatory propagation of the interface. In case of a growing solidification front this offers a transparent scenario for the formation of solute bands in binary alloys, and, taking into account the Mullins-Sekerka instability, of banded structures.

PACS numbers: 68.35.Dv,81.10.Aj,05.70.Np

The interaction of propagating extended defects with a diffusion field frequently leads to oscillations or jerky motions of the defects. A prime example of such an effect is the oscillation of a solidification front, induced by the diffusion of the solute component in a dilute binary alloy, which is growing in the setup of directional solidification. In a large number of metallic materials this leads to the formation of banded structures [1], reflecting a periodic array of layers with high and low solute concentrations where the former ones show a dendritic microstructure. The appearance of similar banding effects has recently been discussed [2] in rapid solidification of colloids.

Layered structures are also generated by the oscillatory nucleation of a solid phase under the action of a diffusion field [3]. A related phenomenon is the oscillatory zoning, observed in solid solutions [4] and in natural minerals [5]. Another notable scenario is that of diffusion-controlled jerky motions of a driven grain boundary [6]. A similar behavior of dislocations in metallic alloys leads to the Portevin-Le Chatelier effect [7], denoting the appearance of jerky plastic deformations. We, finally, mention the oscillatory motion of a crack tip, which is coated by the nucleus of a new phase [8], replacing the attached cloud of a diffusion field.

Theoretical discussions of such effects either are of a phenomenological type, like those in Ref. [7], and partly in Refs. [1] and [2], or they rely on a Fokker-Planck [6], or a diffusion equation with non-equilibrium boundary conditions [9]. In all approaches the source of oscillatory defect motions is identified as an unstable regime where a reduction of the driving force leads to an increase of the defect velocity. Additional information is provided by simulations, based on phase-field models for directional solidification [10] and for nucleation [3] processes.

In the present Letter we introduce an extremely simple but powerful model for the diffusion-induced oscillatory motion of a planar interface, using the language adapted to the directional solidification of a dilute binary alloy. A major advantage of our approach is that it allows a transparent and, to a large extend, analytical evaluation. This includes a readjustment of the stability analysis by Merchant and Davis [11] who discovered an oscillatory instability, similar to that, discussed earlier by Coriell and Sekerka [12]. Also included is a clarifying analysis of the so far barely understood low-velocity sections of the cyclic trajectories, identified by Carrard et al. [1], and by Karma and Sarkissian [9]. The limit-cycle behavior, describing the oscillations of the interface deep inside the unstable regime, is, finally, in remarkable agreement with the simulation results by Conti [10].

Due to the restriction to a planar interface, our model is a one-dimensional version of the capillary-wave model, derived in Ref. [13] from a phase-field model. It is given in dimensionless form by the set of equations

$$H = \frac{\gamma}{2} \int_{-\infty}^{+\infty} dz \, [C(z,t) - U(z - Z(t))]^2 , \quad (1)$$

$$\partial_t Z = p \left(F - \frac{\delta H}{\delta Z} \right) , \quad \partial_t C = \partial_z^2 \frac{1}{\gamma} \frac{\delta H}{\delta C} ,$$

$$F = F_P - m^2 [Z(t) - v_P t]$$

for the interface position $Z(t)$, and for the excess solute concentration $C(z,t)$ relative to its value $C_S \equiv 1$ in the solid phase. The parameter γ measures the miscibility gap $\Delta C = C_L - C_S$ where C_L is the solute concentration in the liquid phase, and p measures the mobility of the interface. From the equilibrium condition $\delta H / \delta C = 0$ it follows that $U(z - Z)$ is the equilibrium-concentration

profile at some fixed temperature T_S. This profile reveals the smooth solid-liquid transition region of the original phase-field model, and is regarded as an input quantity of the model (1). It effectively comprises non-equilibrium effects of sharp-interface descriptions, which are crucial for the behavior in the rapid-growth regime, including the solute-trapping effect [14].

The driving force F includes two quantities, appearing in the simplest scenario of directional solidification. One of them is a constant temperature gradient S, entering the parameter $m^2 \equiv A\,\xi S/T_M$ where, in physical units, ξ measures the width of the interface, visible in the profile $U(\zeta)$, T_M is the melting temperature of the pure solvent, and A is a numerical pre-factor of order one. Adopting from Ref. [10] typical values for S, T_M, ξ, the parameter m^2 is of order 10^{-5}. An independent second quantity is the velocity v_P, applied in pulling the growing crystal in opposite direction to the temperature gradient. The local temperature T_P at the steady-state position $Z(t) = v_P\, t$, finally, determines the fragment $F_P \equiv A(T_S - T_P)/T_M$ of the driving force F.

The resulting equations for $Z(t)$ and $C(z,t)$ read

$$\frac{1}{p}\,\dot{Z}(t) = F_P - m^2[Z(t) - v_P\,t] \qquad (2)$$

$$-\gamma \int_{-\infty}^{+\infty} dz\, U'(z - Z(t))[C(z,t) - U(z - Z(t))] ,$$

$$(\partial_t - \partial_z^2)C(z,t) = -U''(z - Z(t)) .$$

For steady-state boundary conditions $C(z = \pm\infty) = 0$, they have the stationary solutions $Z(t) = v_P\,t$, and $C(z,t) = C_P(z - v_P\,t; v_P)$, resulting in the relations

$$\frac{1}{p}\,v_P = F_P + G_P(v_P) - G_P(0) , \qquad (3)$$

$$G_P(v_P) \equiv -\gamma \int_{-\infty}^{+\infty} d\zeta\, U'(\zeta)\, C_P(\zeta; v_P) ,$$

$$C_P(\zeta; v_P) = \int_{-\infty}^{\zeta} d\zeta'\, U'(\zeta')\, \exp[v_P(\zeta' - \zeta)] .$$

We are primarily interested in the late-stage behavior of non-stationary solutions $Z(t)$, and, therefore, look for a solution $C(z,t)$ of the last equation in Eqs. (2), obeying the boundary condition $C(z, -\infty) = 0$. This leads to the expression

$$C(z,t) = \int_{-\infty}^{t} dt' \int_{-\infty}^{+\infty} dz'\, \partial_{z'}\mathcal{G}(z - z', t - t')$$
$$\cdot U'(z' - Z(t')) , \qquad (4)$$

involving the Green function

$$\mathcal{G}(z,t) = \int_{-\infty}^{+\infty} \frac{dk}{2\pi}\, \exp(-k^2 t + ik\, z) . \qquad (5)$$

After the substitutions $\zeta \equiv z - Z(t), \zeta' \equiv z' - Z(t')$, and expansion of $Z(t')$ around $Z(t)$, we obtain

$$\mathcal{G}(\zeta - \zeta' + Z(t) - Z(t'), t - t') = \qquad (6)$$

$$\int_{-\infty}^{+\infty} \frac{dk}{2\pi}\, \exp\left[-k^2(t - t') + ik(\zeta - \zeta') + ik(t - t')v(t)\right]$$

$$\cdot \exp\left[-ik \sum_{n \geq 2} \frac{(-1)^n}{n!}(t - t')^n \partial_t^{n-1} v(t)\right]$$

where $v(t) \equiv \dot{Z}(t) = v_P + \dot{h}(t)$.

If one temporarily applies the scaling transformations $h \to m^{-2}h, \partial_t \to m^2\partial_t$, one observes that, whereas $v(t)$ remains unchanged, a factor m^{2n-2} is attached to the contributions $\propto \partial_t^{n-1}v(t)$. Therefore, with increasing n these terms are progressively negligible in Eq. (6) due to the smallness of m^2. Neglecting all terms of order $n \geq 2$, we encounter the quasi-stationary approximation, which is often used in phenomenological approaches. As we shall see, however, a proper understanding of oscillatory motions of the interface requires to incorporate the term of order $n = 2$.

Evaluation of Eqs. (4) - (6) then leads to the expression

$$C(z,t) = C_P(\zeta; v) + \dot{v}\,\frac{1}{2}\frac{\partial^2}{\partial v^2}\frac{1}{v}[C_P(\zeta; v) + C_P(\zeta; 0)] \quad (7)$$

with $C_P(\zeta; v_P)$ determined by the last line in Eqs. (3). Insertion of this result into the first equation in Eqs. (2) yields the relation

$$\frac{1}{p}\,v = F_P - m^2(Z - Z_P) \qquad (8)$$

$$+\, G_P(v) - G_P(0) + \dot{v}\frac{1}{2}\frac{\partial^2}{\partial v^2}\frac{1}{v}[G_P(v) + G_P(0)]$$

with $G_P(v)$ following from the second line in Eqs. (3). For $v = v_P$ the result (8) consistently reduces to the first equation in Eqs. (3). Subtracting the latter from Eq. (8), we, finally, find for the displacement $h(t) \equiv Z(t) - Z_P(t)$ the differential equation

$$M(\dot{h}(t))\,\ddot{h}(t) + R(\dot{h}(t)) + m^2\,h(t) = 0 \qquad (9)$$

where we have introduced the mass and friction functions

$$M(\dot{h}) \equiv -\frac{1}{2}\frac{\partial^2}{\partial v_P^2}\left[\frac{G_P(v_P + \dot{h}) + G_P(0)}{v_P + \dot{h}}\right] ,$$

$$R(\dot{h}) \equiv \frac{1}{p}\,\dot{h} - G_P(v_P + \dot{h}) + G_P(v_P) . \qquad (10)$$

Eq. (9) has the typical appearance of a nonlinear damped oscillator, and represents one of the central results of the
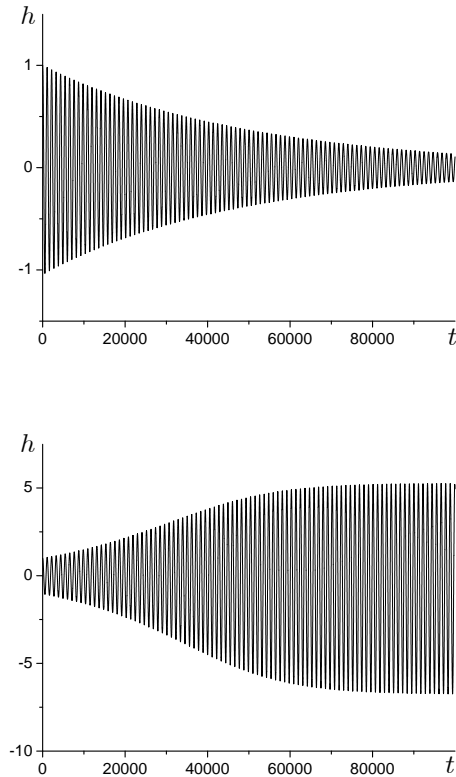
FIG. 1: Numerical solutions $h(t)$ for $\gamma = 0.01$, $p = 100$, $m = 0.003$, approaching the value $h = 0$ for $v_P = 0.522$, and a limit cycle for $v_P = 0.520$.

present Letter. We mention that, due to the singular dependence of $M(\dot{h})$ on $v_P + \dot{h}$, the differential equation (9) is only valid below the crossover line $m^2 \propto (v_P + \dot{h})^3$.

In order to check the stability of the obvious solution $h(t) = 0$, we linearize Eq. (9) in h(t), which, due to the definitions (10) and the first line in Eqs. (3), yields

$$M(0)\ddot{h} + F_P'(v_P)\dot{h} + m^2 h = 0 . \qquad (11)$$

In this ordinary oscillator equation the friction coefficient can change sign at some critical velocity v_C, defined by $F_P'(v_C) = 1/p - G_P'(v_C) = 0$. A similar stability limit has been found by Cahn in grain-boundary motion [6].

For quantitative discussions of the behavior of $h(t)$ we now adopt the specific model

$$U(\zeta) = \Theta(-\zeta)\exp\zeta + \Theta(\zeta)[2 - \exp(-\zeta)] , \qquad (12)$$

derived in Ref. [13] from a double-parabola phase-field model. Then, solving the integrals in Eqs. (3), one finds

$$G_P(v) = -\gamma\frac{v + 2}{(v + 1)^2} , \qquad (13)$$

which determines all terms in the oscillator equation (9).

The resulting numerical solutions for $h(t)$ above and below the Cahn threshold v_C are shown in Fig. 1 where the approach to a limit cycle in the unstable regime is clearly visible. For small distances $|v_P - v_C|/v_C \ll 1$ the envelopes of these curves can be calculated analytically by the Bogoliubov-Mitropolsky method [15]. To leading order one finds

$$h(t) = a(t)\cos\psi(t) \qquad (14)$$

where $\psi(t)$ is a rapidly oscillating phase, and $a(t)$ is an amplitude, obeying the differential equation

$$\frac{da}{dt} = -\rho_1 a - \rho_3 a^3 , \qquad (15)$$

with $\rho_1 \equiv r_1(v_P - v_C)$, and the parameters r_1, ρ_3 fixed by the values of γ, p. The solution of Eq. (15) reads

$$a(t) = a_0\left\{\left[1 + \frac{\rho_3}{\rho_1}a_0^2\right]\exp\left[2\rho_1 t\right] - \frac{\rho_3}{\rho_1}a_0^2\right\}^{-1/2} , \qquad (16)$$

which for $\rho_1 > 0$ and $\rho_1 < 0$ describes the envelopes in Fig. 1. The asymptotic value of the limit-cycle amplitude shows the critical behavior $a(\infty) = \sqrt{-\rho_1/\rho_3}$.

The numerically obtained limit-cycle trajectories of the quantities $h(t)$, $\dot{h}(t)$, $C(Z(t), t)$ deep inside the unstable regime are displayed in Fig. 2. They also inform on the local temperature at the oscillating interface, since this is measured by the quantity $m^2 h(t)$. The pronounced oscillations of the solute concentration at the interface $C(Z(t), t)$ reflects the appearance of solute bands. From the curves in Fig. 2, which in part are remarkably close to the findings by Conti in Ref. [10], one concludes that the high- and low-concentration layers are connected by large-acceleration segments, explaining the sharpness of the interfaces between these layers.

In order to explore the possible formation of dendritic ripples, one has to consider perturbations of the form $h(\mathbf{x}, t) = \hat{h}(\mathbf{q}, \omega)\exp(i\mathbf{q}\cdot\mathbf{x} + \omega t)$ in a three-dimensional version of the model (1). In view of the almost stationary behavior of $\dot{h}(t)$ in Fig. 2 at low velocities, we choose, as an approximation, $\dot{Z}(t) = v_P$ as a reference velocity. Following Ref. [13], we then find the dispersion relation

$$\frac{\omega}{p} + q^2 + m^2 - v_P[G_P(v_P + \lambda) - G_P(v_P)] =$$

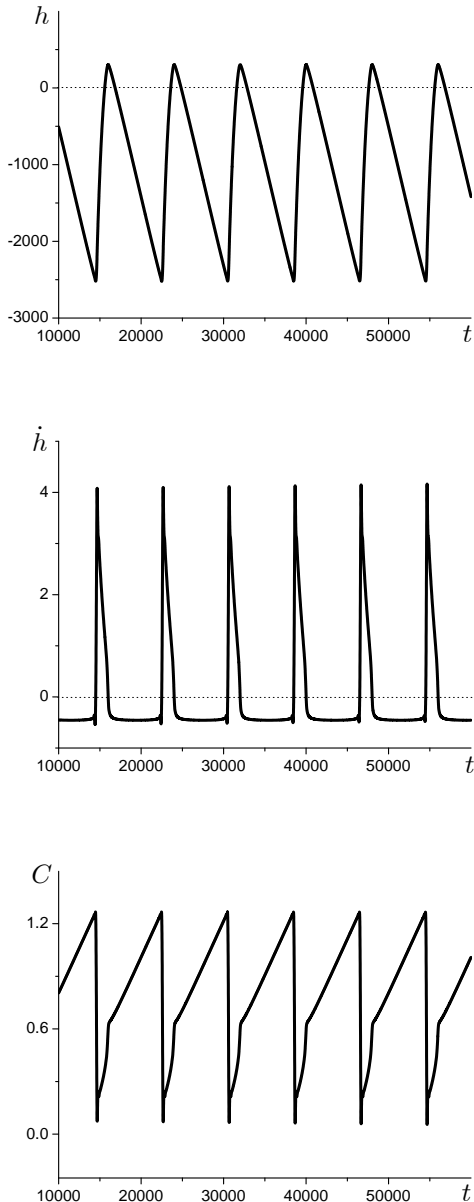$$\frac{\lambda^2 - q^2}{v_P + 2\lambda}[G_P(v_P + \lambda) + G_P(\lambda)] , \qquad (17)$$

FIG. 2: Trajectories of $h(t), \dot{h}(t), C(Z(t), t)$ in the unstable regime for $\gamma = 0.02$, $p = 100$, $m = 0.003$, and $v_P = 0.5$.
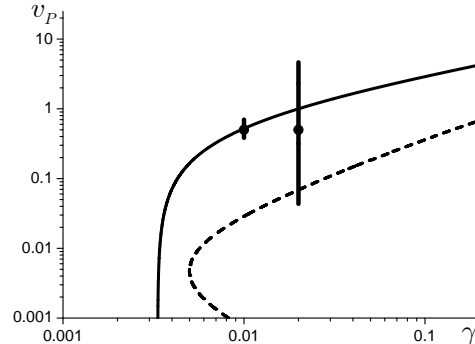

FIG. 3: Neutral stability curves, enclosing the regions of the Cahn (solid line), and of the Mullins-Sekerka instability (dashed line). The vertical lines are projections of limit cycles at $\gamma = 0.01$ and $\gamma = 0.02$, both at $p = 100, m = 0.003$ and $v_P = 0.5$.

metallic alloys. The other small cycle in Fig. 3 generates layers of precipitation-free periodic solute concentrations.

The most obvious generalization of our procedure is to explore the formation of non-planar layering effects, which also is a field for experimental investigations. A typical example of such an effect is the oscillatory growth of a spherical nucleus, which has been discussed on the basis of a phase-field model in Ref. [3], and which we are going to reconsider within our approach.

with $\lambda \equiv -(v_P/2) + \sqrt{(v_P/2)^2 + \omega + q^2}$ where the term m^2 is the only new element. The wave-number threshold q_c for the Mullins-Sekerka instability [16] is determined by the relations $\omega_1(q_c) = \omega_1'(q_c) = 0$. By elimination of q_c from these equations one generates the neutral-stability boundary of the instability in form of a function $v_P(\gamma)$, with a parametric dependence on m.

In Fig. 3 the projection of the limit cycle, belonging to Fig. 2, enters the Mullins-Sekerka unstable regime at low velocities where the interface develops a dendritic microstructure, a typical feature of banded structures in

[1] M. Carrard, M. Gremaud, M. Zimmermann, W. Kurz, Acta metall. mater. **40**, 983 (1992).
[2] J. A. W. Elliott, S. S. L. Peppin, Phys. Rev. Lett. **107**, 168301 (2011).
[3] T. Kyu, H.-W. Chiu, A. J. Guenthner, Y. Okabe, H. Saito, T. Inoue, Phys. Rev. Lett. **83**, 2749 (1999).
[4] A. Putnis, L. Fernandez-Diaz, M. Prieto, Nature **358**, 743 (1992).
[5] M. Shore, A. D. Fowler, Can. Mineral. **34**, 1111 (1996).
[6] J. W. Cahn, Acta Metal. **10**, 789 (1962).
[7] M. A. Lebyodkin, Y. Brechet, Y. Estrin, L. P. Kubin, Phys. Rev. Lett. **74**, 4758 (1995).
[8] A. Boulbitch, A. L. Korzhenevskii, Phys. Rev. Lett. **107**, 085505 (2011).
[9] A. Karma, A. Sarkissian, Phys. Rev. Lett. **68**, 2616 (1992); Phys. Rev. E **47**, 513 (1993).
[10] M. Conti, Phys. Rev. E **58**, 2071 (1998); Phys. Rev. E **58**, 6101 (1998).

[11] G. J. Merchant, S. H. Davis, Acta metall. mater. **38**, 2683 (1990).

[12] S. R. Coriell, R. F. Sekerka, J. Cryst. Growth. **61**, 499 (1983).

[13] A. L. Korzhenevskii, R. Bausch, R. Schmitz, Phys. Rev. E 83, 041609 (2011).

[14] M. J. Aziz, W. J. Boettinger, Acta metall. mater. **42**, 527 (1994).

[15] N. N. Bogoliubov, Y. A. Mitropolsky, *Asymptotic Methods in the Theory of Nonlinear Oscillations*, (Gordon and Breach Science Publishers, New York, 1961).

[16] W. W. Mullins, R. F. Sekerka, J. Appl. Phys. **35**, 444 (1964).